analytical chemistry

pubs.acs.org/ac Article

Ultrasensitive Electrochemiluminescence Biosensor Based on Closed Bipolar Electrode for Alkaline Phosphatase Detection in Single Liver Cancer Cell

Xiao-Yan Yang, Yi-Yan Bai, Yue-Yue Huangfu, Wen-Jing Guo, Yan-Ju Yang, Dai-Wen Pang, and Zhi-Ling Zhang*

Cite This: *Anal. Chem.* 2021, 93, 1757−1763 Read Online

ACCESS | Metrics & More | Article Recommendations | Supporting Information

ABSTRACT: An ultrasensitive electrochemiluminescence (ECL) biosensor was proposed based on a closed bipolar electrode (BPE) for the detection of alkaline phosphatase (ALP). For most of the BPE−ECL biosensors, an effective signal amplification strategy was the key to enhance the sensitivity of the system. Herein, the signal amplification strategy of the enzyme catalysis was utilized in the BPE−ECL system. Au nanoparticles (NPs) were electrodeposited on the cathode surface of the ITO electrode to improve the stability and sensitivity of the signal. Compared with the previous BPE−ECL biosensors, the sensitivity was increased by at least 3 orders of magnitude. The biosensor showed high sensitivity and specificity of ALP detection with a detection limit of as low as 3.7 aM. Besides, it was further applied to the detection of ALP in different types of cells and successfully realized ALP detection in single Hep G2 cell, which had a huge application prospect in single biomolecule detection or single cell analysis.

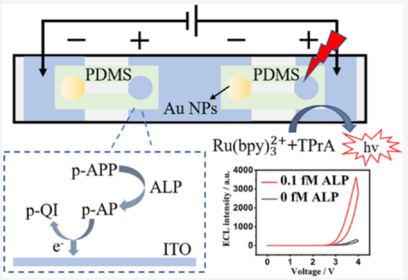

In the past two decades, bipolar electrodes (BPEs) have emerged in the field of analysis due to easy control, no direct electrical contact,[1] easy miniaturization, and portability and have attracted the attention of many scientific researchers.[2−5] A common strategy used to study bipolar electrodes is to combine electrochemiluminescence (ECL)[6] based on their outstanding advantages of high detection sensitivity,[7] no need for excitation light source,[8] and simple instrumentation.[9] The ECL technology is a combination of chemiluminescence and electrochemistry, which not only has the sensitivity and wide dynamic range of chemiluminescence but also holds the simplicity and facility of electrochemical detection.[10,11] The ideal combination of closed bipolar electrodes and electrochemiluminescence technology has resulted in rapid development for application in biological analysis.[12] At present, electrochemiluminescence biosensors based on closed bipolar electrodes are being successfully utilized to detect biomolecules (DNA,[13] mucin-1,[14] prostate antigen[15]), small molecules (H_2O_2,[16] $K_3Fe(CN)_6$,[17,18] glucose[3]), cancer cells,[19] etc.

In most BPE−ECL systems, the electroactive substance was directly detected, and the detection limit reached the detection level of μM.[20,21] However, the exploration of biomedicine has reached the single-molecule and single-cell levels in recent years,[22] the level of μM was far from meeting the requirements of detection. For this reason, researchers have made great efforts in signal amplification to improve the sensitivity of detection.[23,24] So far, effective signal amplification strategies have made great progress, which are divided into two categories. The first one is the signal amplification of nanomaterials, which are modified on the surface of the bipolar electrode to improve the electron-transfer capacity of the electrode surface, thereby improving the response performance of the biosensor. Wang's group developed a full-featured ECL sensing platform based on a multichannel closed bipolar system.[25] Pt was electrodeposited on the surface of the BPE cathode to improve the signal stability. At the same time, compared to the unmodified situation, it also improved the sensitivity of detection. Besides, the signal labeling of nanomaterials could also be used to enhance the detection signal. Xu's group reported a BPE−ECL biosensor for the detection of prostate antigen (PSA). At the cathode of BPE, Th@SiO_2 nanoparticles were introduced as both recognition probes for PSA and signal amplification indicators. The sensitivity was further improved and the detection limit was 0.1 pg/mL (3 fM), which fulfilled the clinic requirements of PSA detection.[26] The second category is the enzyme catalysis, which directly amplifies the detection signal through the catalytic amplification effect of the enzyme on the substrate.[27] Xu and co-workers combined the enzyme-catalyzed signal

Received: October 26, 2020
Accepted: December 17, 2020
Published: December 29, 2020

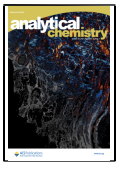

https://dx.doi.org/10.1021/acs.analchem.0c04517
Anal. Chem. 2021, 93, 1757−1763

amplification strategy with the BPE−ECL system. Glucose was catalyzed by glucose oxidase to form H_2O_2. Through the reduction reaction of H_2O_2, highly sensitive detection of PSA was achieved.[28] These signal amplification strategies impelled the detection limit of the system reaching the fM level, which greatly improved the sensitivity of detection and provided the possibility for the detection of a single molecule and a single cell.

Enzyme-induced metallization refers to the process in which metal ions are reduced to the metal elements under the catalysis of enzymes.[29] It not only combines the specificity of enzyme-catalyzed reaction but also has the characteristics of the high sensitivity of gold-labeled silver staining.[30] Combined with enzyme-induced metallization, the colorimetric method was utilized to quickly and easily achieve highly sensitive detection of the target.[31,32] Combined with electrochemistry, the method also realized the detection of a single alkaline phosphatase (ALP) molecule.[33,34] Based on this result, for improving the sensitivity of the BPE−ECL system to achieve single molecule or single cell detection, enzyme-induced metallization was considered in the BPE−ECL system. Ultrasensitive detection of ALP was achieved through the catalytic amplification effect of ALP on the substrate and further applied to the detection of ALP in the single cell.

Herein, an electrochemiluminescence biosensor based on a closed bipolar electrode for ALP detection was proposed. Enzyme-catalyzed signal amplification strategy was combined with the BPE−ECL system. Compared with the previous BPE−ECL biosensors, the sensitivity was remarkably improved. It could achieve the detection level of aM and could be further applied to the ALP detection in a single Hep G2 cell. Besides, the constructed BPE−ECL system could realize anode oxidation and anode ECL signal output. Compared with the previous BPE−ECL systems, it broadened the scope of detection and could achieve oxidation detection.

EXPERIMENTAL SECTION

Reagents and Instruments. Alkaline phosphatase (ALP, Calf intestine) and $Ru(bpy)_3^{2+}$ were purchased from Sigma-Aldrich (St. Louis, MO). The *p*-aminophenyl phosphate monohydrate (*p*-APP) was obtained from Santa Cruz Biotechnology, Inc. Tripropylamine (TPrA) and 4-aminophenol (*p*-AP) were received from Aladdin (Shanghai, China). Liver cancer cells (Hep G2 cells) and breast cancer cells (MCF-7 cells) were purchased from the China Center for Type Culture Collection. The poly(dimethylsiloxane) (PDMS) and curing agent were purchased from GE (GE Toshiba Silicones. Co., Ltd., Japan). All other chemical reagents were purchased from Sinopharm Chemical Reagent Co., Ltd. (Shanghai, China). Ultrapure water was obtained from a Millipore water purification system (≥18 MΩ/cm, Milli-Q, Millipore).

All of the ECL experiments were measured with the MPI-E electrochemiluminescence analytical system (Xi'an Remex Analytical Instrument Co., Ltd. China). SEM (ZEISS SIGMA FESEM) was used to characterize the morphology of gold nanoparticles modified closed bipolar electrode. Cells were selected under an inverted fluorescence microscope (TiU, Nikon).

Preparation of the Closed Bipolar Electrode. The existing photolithography technology in our laboratory was used to prepare a closed bipolar electrode.[33] First, the photoresist (AZ4620) was spin-rotated evenly on the ITO glass (7.5 cm × 2 cm) and exposed to ultraviolet light for 30 s with the photomask. When an AZ developer was developed, the photoresist in the exposed area was removed. Next, the ITO glass was placed in concentrated HCl to remove the ITO conductive layer on the surface of the area without a photoresist. After that, ethanol was used to wash away the remaining photoresist on the surface of the glass. The fabrication of a closed bipolar electrode is shown (Figure 1).

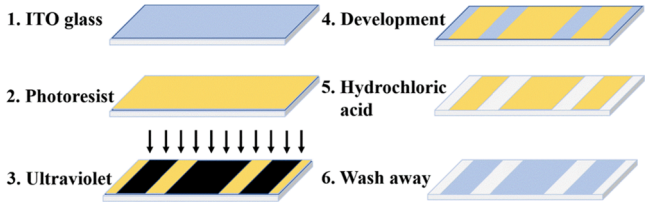

Figure 1. Fabrication of a closed bipolar electrode by the soft photolithography technology.

It consisted of three ITO electrodes, whose lengths were 1.5, 2.5, and 1.5 cm. There was a gap of 0.7 cm between each other. The desktop homogenizer was set at the speed and time in advance. PDMS (10:1 w/w RTV615A/RTV615B) was spin-rotated evenly on the silicon chip and baked at 75 °C for 4 h. Then, the solid PDMS was peeled off from the silicon chip. It was punched with 6 mm diameter small holes and a straight channel which was 0.7 cm in length connected to two small holes. Finally, the patterned PDMS film was bonded on the surface of the bipolar electrode.

Fabrication of Au NP-Modified Closed Bipolar Electrode. Gold nanoparticles were deposited on the bipolar electrode by electrochemical deposition.[35] One hundred microliters of 1% chloroauric acid solution was added to cells on each side and a constant voltage was applied on both ends of driving electrodes for 180 s. After the reaction was completed, the electrode surface was rinsed with ultrapure water and dried with N_2; thus, a bipolar electrode modified with Au NPs was obtained.

Ultrasensitive ALP Detection. The closed bipolar electrode modified with Au NPs was applied to detect ALP. The ECL detection reagents ($Ru(bpy)_3^{2+}$/TPrA, 2.5/60 mM) in PBS buffer (100 μL, 0.1 M, pH 7.2) were introduced into the reporting cell. Different concentrations of ALP and 3 mM *p*-APP in diethanolamine were mixed well and incubated at 37 °C for 30 min and then injected into the sensing cell for ECL detection. The ECL signal was obtained by applying cyclic voltammetry (CV) from 0 to 4.0 V on both ends of the driving electrodes with a 200 mV/s scanning rate. The voltage of the photomultiplier tube (PMT) was set at 800 V during the whole detection.

ALP Detection in Cancer Cells. The method was applied to the ALP detection in cancer cells; 10^6 Hep G2 cells were collected under a microscope. After being lysed, the Hep G2 cells were centrifuged at 4 °C with 10 000 rpm for 10 min and the supernatant was collected. MCF-7 cells (10^4) and 10^4 Hep G2 cells were compared for the ALP content. Besides, different numbers of Hep G2 cells were detected in the anode of a bipolar electrode to obtain the ECL responses.

RESULTS AND DISCUSSION

Working Principle for the Closed Bipolar Electrode. In most BPE−ECL systems, the conventional ECL detection

https://dx.doi.org/10.1021/acs.analchem.0c04517
Anal. Chem. 2021, 93, 1757−1763

reagents participated in the oxidation reaction at the anode of the bipolar electrode, while the reactants could only be reduced at the cathode of the bipolar electrode, which had certain restrictions on target detection. In this work, the reactant was oxidized at the anode of the bipolar electrode. The ECL signal was obtained on the anode of the driving electrode. As shown in Scheme 1, the Au NP-modified

Scheme 1. Schematic Diagram for the ALP Detection with Electrochemiluminescence Biosensor Based on Closed Bipolar Electrode

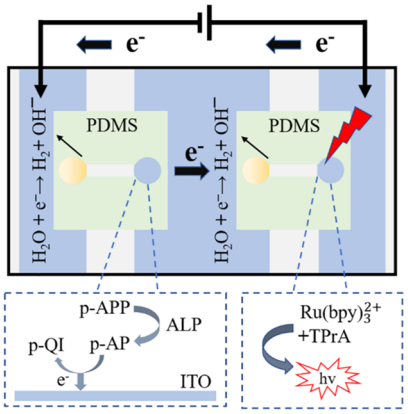

electrode (Au-ITO) could provide a stable potential for decreasing the impact of the driving electrodes.[36] When the voltage was applied across the driving electrodes, a close-circuit was constructed through electron transfer and ion transfer in the solution. The ALP catalyzed the substrate *p*-APP to form 4-aminophenol (*p*-AP). *p*-AP was oxidized at the anode of the bipolar electrode, and the ECL signal was excited at the anode of the driving electrode. The detection of ALP was converted to the detection of the oxidation reaction of *p*-AP and converted to the detection of the ECL signal finally.

Ultrasensitive detection of ALP was realized based on the efficient signal amplification strategy of an enzyme-catalyzed reaction. The control groups and the experimental group were designed to measure the feasibility of the method. Under the condition of ALP catalysis, *p*-AP was generated by *p*-APP. Without ALP, the enzyme-catalyzed reaction could not be carried out and the ECL signal was weak (Figure 2a). In the absence of *p*-APP, a weak ECL response was obtained (Figure 2b). Only when both *p*-APP and ALP existed, there was a strong ECL signal (Figure 2c). It turned out that this method could be adopted to the detection of ALP.

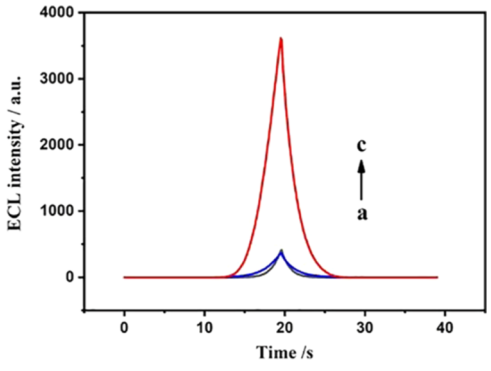

Figure 2. ECL responses of different solution compositions in the anode of the bipolar electrode: (a) *p*-APP, (b) ALP, and (c) ALP + *p*-APP.

According to the enzyme reaction mechanism, the electrode reactions were as follows

$$p - \mathrm{APP} \xrightarrow{\mathrm{ALP}} p - \mathrm{AP} + \mathrm{PO_4^{3-}} \quad (1)$$

Bipolar electrode anode reaction:

$$p - \mathrm{AP} - \mathrm{e^-} \rightarrow p - \mathrm{QI} + \mathrm{H^+} \quad (2)$$

Bipolar electrode cathode reaction:

$$4\mathrm{H_2O} + 4\mathrm{e^-} \rightarrow 2\mathrm{H_2} + 4\mathrm{OH^-} \quad (3)$$

Driving electrode cathode reaction:

$$4\mathrm{H_2O} + 4\mathrm{e^-} \rightarrow 2\mathrm{H_2} + 4\mathrm{OH^-} \quad (4)$$

Driving electrode anode reaction:

$$\begin{cases} \mathrm{Ru(bpy)_3^{2+}} - \mathrm{e^-} \rightarrow \mathrm{Ru(bpy)_3^{3+}} \\ \mathrm{TPrA} - \mathrm{e^-} \rightarrow \mathrm{TPrA^{+\cdot}} \\ \mathrm{TPrA^{+\cdot}} \rightarrow \mathrm{TPrA^{\cdot}} + \mathrm{H^+} \\ \mathrm{Ru(bpy)_3^{3+}} + \mathrm{TPrA^{\cdot}} \rightarrow [\mathrm{Ru(bpy)_3^{2+}}]^* \\ [\mathrm{Ru(bpy)_3^{2+}}]^* \rightarrow \mathrm{Ru(bpy)_3^{2+}} + h\nu \end{cases} \quad (5)$$

In short, the constructed system could realize oxidation detection of the anode on the bipolar electrode with ECL signal was obtained at the anode of the driving electrode and could be further successfully applied to the detection of ALP.

Au NPs Enhanced the Stability and Sensitivity of the System. Gold nanoparticles were deposited on the cathode surface of the electrode by applying a constant voltage of 3 V on both ends of the driving electrodes for 180 s. Figure 3A is a schematic diagram of a closed bipolar electrode, the yellow part meant gold nanoparticles. SEM was used to characterize the morphology of Au NPs on the surface of the electrode. The result showed that Au NPs had a uniform particle size and a good dispersion (Figure 3B). Figure 3C shows that the comparison of the electrode modified with Au NPs and bare ITO electrode. The ECL intensities of the electrode modified with Au NPs did not change (RSD: 1.59%) after three renewal solutions, while the ECL intensities of the bare ITO electrode changed significantly (RSD: 74.19%). By applying cyclic voltammetry (CV) from 0 to 4.0 V, the component SnO_2 in the bare ITO electrode was destroyed at the cathode, which was reduced and the cathode turned black, as observed through the naked eye, causing the ECL signal to become unstable. The Au NPs protected the electrode from SnO_2 reduction. Besides, the deposition of Au NPs made the electrode exhibit better conductivity, and the ECL response was enhanced at the anode. Figure 3C displays that the stability of the Au NP-modified electrode was better than that of the bare ITO electrode, and the sensitivity of the Au NP-modified electrode was higher than that of the bare ITO electrode. Five closed bipolar electrodes modified with Au NPs were randomly selected to detect the ECL signal. It could be seen that the ECL signals were stable (RSD: 1.76%) and had good repeatability (Figure 3D). The above results showed that the closed bipolar electrode modified with Au NPs had a good performance, with high sensitivity and stability.

Optimization of the Experiment Conditions. The driving voltage, the concentration of the substrate *p*-APP, the

https://dx.doi.org/10.1021/acs.analchem.0c04517
Anal. Chem. 2021, 93, 1757−1763

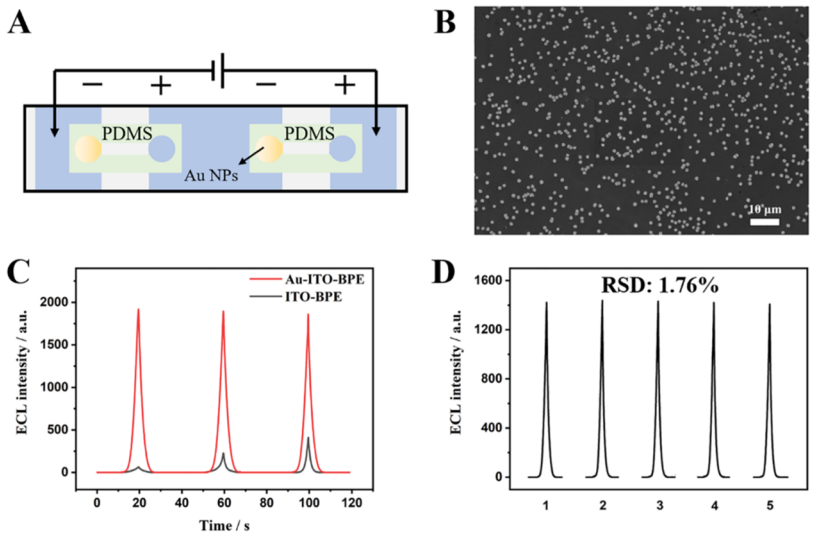

Figure 3. (A) Schematic diagram of the Au NP-modified bipolar electrode. (B) SEM image of Au NPs. (C) Comparison of the Au NP-modified bipolar electrode and the bare bipolar electrode with 0.02 fM ALP after renewing the solutions (0, 40, 80 s). (D) ECL responses of five parallel closed bipolar electrodes with 0.01 fM ALP.

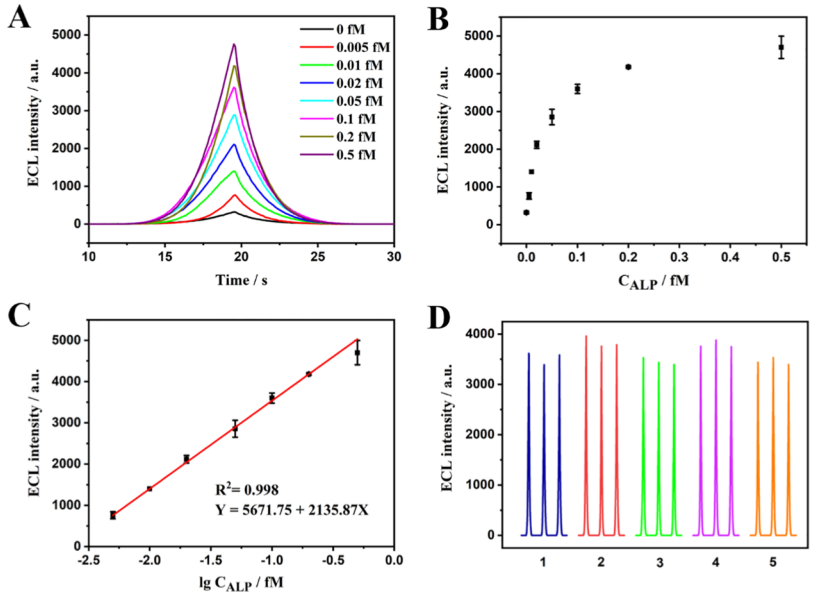

Figure 4. (A) ECL intensities of ALP at different concentrations: 0, 0.005, 0.01, 0.02, 0.05, 0.1, 0.2, and 0.5 fM. The ECL signals were recorded after 30 min of incubation at 37 °C. (B) Scatter plot for the ECL responses of ALP (n = 3). (C) Linear relationship between the ECL intensities and the concentrations of ALP from 0.005 to 0.5 fM. (D) Reproducibility of the ECL biosensor with 0.1 fM ALP (RSD = 5.2%).

concentration of TPrA, and the incubation time were optimized to have a better performance of ECL. The driving voltage was optimized using linear sweep voltammetry from 0 to 5.0 V (Figure S1, Supporting Information). When the voltage exceeded 4.2 V, the current response (Figure S1A) and the ECL response (Figure S1B) rose quickly with the increase of voltage. The cathode turned black as observed through the naked eye, which showed that SnO_2, the surface component of the ITO electrode, participated in the cathode reaction. Besides, there was an ECL peak between 0 and 4.0 V, and the ITO electrode composition was not destroyed. Therefore, the driving voltage of 0−4.0 V was selected as the optimal condition.

The detection conditions were optimized to improve the sensitivity of ALP detection. p-APP was catalyzed by ALP, and its concentration determined the final production of p-AP. The concentration of p-APP was optimized to obtain the maximum signal-to-background ratio of detection, and the optimal reaction concentration of p-APP was 3 mM (Figure S2A, Supporting Information).

Then, as a co-reactant of $Ru(bpy)_3^{2+}$, the concentration of TPrA played a key role in the intensity of ECL. To improve the signal-to-background ratio of detection, the concentration of TPrA was optimized, and the optimal reaction concentration of TPrA was 60 mM (Figure S2B, Supporting Information).

Finally, the enzyme reaction time also affected the ECL response. The signal-to-back ratio increased with the incubation time, and it reached 30 min and then stabilized. The optimal reaction time was 30 min (Figure S2C, Supporting Information).

Ultrasensitive ALP Detection. Electrochemiluminescence biosensor based on the closed bipolar electrode was

https://dx.doi.org/10.1021/acs.analchem.0c04517
Anal. Chem. 2021, 93, 1757−1763

constructed for ultrasensitive ALP detection. The target was added to the anode of the bipolar electrode, and the ECL responses were performed by the scanning potential from 0 to 4.0 V under the optimal reaction conditions (Figure 4A). The ECL intensities increased with the concentration of the ALP (Figure 4B). There was a good linear range from 0.005 to 0.5 fM of ALP with a detection limit of 3.7 aM (Figure 4C). The linear equation was $I = 5671.75 + 2135.87 \times \lg C$ with $R^2 = 0.998$. The high sensitivity mainly depended on efficient signal amplification strategies. (1) By combining enzyme-catalyzed signal amplification strategy with the BPE−ECL system, through the catalytic amplification effect of ALP on the substrate, the production of *p*-AP was used indirectly to express the concentration of ALP, rather than directly detecting the content of ALP. The detection of enzyme concentration through enzyme-catalyzed reaction had more signal amplification effect than the direct detection of the enzyme molecule itself (Figure 2). Also, a further experiment was established by extending the time of enzyme catalysis from 30 min to 1 h due to longer incubation time; the enzyme-catalyzed reaction was more sensitive and could detect as low as 0.5 aM ALP (Figure S3, Supporting Information). This value was an order of magnitude higher than that of the original system, which showed that the enzyme catalysis could amplify the signal and thus the sensitivity of the method has been improved. (2) Au NP-modified bipolar electrode had high sensitivity and could greatly amplify the ECL signal (Figure 3C). Ultrasensitive detection of ALP was realized by combining enzyme-catalyzed reaction and signal amplification of Au NPs. Compared with other reported methods with ECL biosensors based on a closed bipolar electrode (Table S1, Supporting Information), this method could achieve the detection level of aM, whose sensitivity was increased by at least 3 orders of magnitude. When only *p*-AP was added to the sensing cell, the ECL signal had a corresponding relationship with the concentration of *p*-AP by the scanning potential from 0 to 4.0 V. The ECL signal increased with the concentration of *p*-AP, which further confirmed the principle. It could detect 1 fM *p*-AP. The catalytic amplification of the enzyme allowed ALP to be detected at an aM level, which also illustrated the efficient signal amplification strategy of enzyme catalysis (Figure S4, Supporting Information). Five different batches of Au NP-modified bipolar electrodes were randomly selected to test the performance of the biosensor. The reproducibility of the ECL biosensor with 0.1 fM ALP is shown in Figure 4D. The relative standard deviation (RSD) was 5.2%, which showed that the constructed biosensor had good stability and excellent reproducibility.

In addition, 10 mM glucose, 10 mM urea, 1 mM cytochrome *c*, and 1 μM thrombin were introduced as negative control groups, whose concentrations were 10^9 times higher than the concentration of ALP. Only in the presence of ALP, the ECL signal was strong and the other four groups of ECL signals were weak (Figure 5). The result demonstrated that the BPE−ECL biosensor had high specificity.

ALP Detection in Cancer Cells. The detection of the target in the actual sample was an important index to evaluate the analytical performance of the biosensor. As shown in Table 1, 0.02, 0.05, and 0.1 fM ALP were spiked into 100 Hep G2 cells, and the results were in good agreement with the total amount. The recovery rate of the standard addition was from 97.8 to 103.3%, which showed that the method was applicable for the detection of ALP in cancer cells.

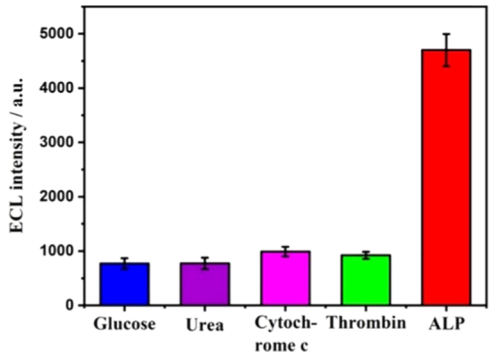

Figure 5. Specificity of ALP detection (negative control groups: glucose, urea, cytochrome *c*, thrombin).

Table 1. Detection of ALP in 100 Hep G2 Cells ($n = 3$)

sample	added (fM)	found (fM)	recovery (%)	RSD (%)
1	0	0.0072		4.3
2	0.02	0.0270	99.0	3.7
3	0.05	0.0561	97.8	6.1
4	0.1	0.1105	103.3	3.5

The content of ALP in different types of cells was different. The same number of Hep G2 cells and MCF-7 cells were selected to detect the content of ALP. It was found that the content of ALP in the 10^4 MCF-7 cells was much less than that in the 10^4 Hep G2 cells (Figure 6A), which was consistent with the literature report.[33] Na_3VO_4 was a commonly used inhibitor of ALP, which was used to inhibit the ALP activity in Hep G2 cells. The ECL signal was significantly lower than the group without Na_3VO_4. The above results showed that the biosensor had good sensitivity and accuracy.

Besides, the biosensor was applied to the detection of ALP in different quantities of Hep G2 cells. The ECL signals increased with the number of cells. Compared with that of the blank control group, the detection of ALP in the 100 Hep G2 cell sample showed a significant ECL signal (Figure 6B). Furthermore, to facilitate the detection of ALP in a single cell, the conditions have been expanded by extending the incubation time from 30 min to 1 h and reducing the volume of the reaction system from 100 to 50 μL to achieve the quantitative analysis of ALP in a lower cell number. First, the concentration standard curve of ALP was obtained after the conditions had been changed (Figure S3, Supporting Information), and it was found that as low as 0.5 aM ALP was detected, which was 15 ALP molecules in the system. The sensitivity had been further improved, which provided the possibility for single cell detection. Then, a certain number of cells were selected under a microscope and lysed for ALP detection. Overall, the ECL signals increased with the number of cells (Figure 6C,D), and the content of ALP had a corresponding relationship with the number of cells. However, the ECL signal of the same number of cells had a big deviation, which might be that the ALP content of individual cells was not the same, indicating that there was heterogeneity among individual cells. The biosensor provided the possibility of single cell detection, promoted the development of single biomolecule detection or single cell analysis.

https://dx.doi.org/10.1021/acs.analchem.0c04517
Anal. Chem. 2021, 93, 1757−1763

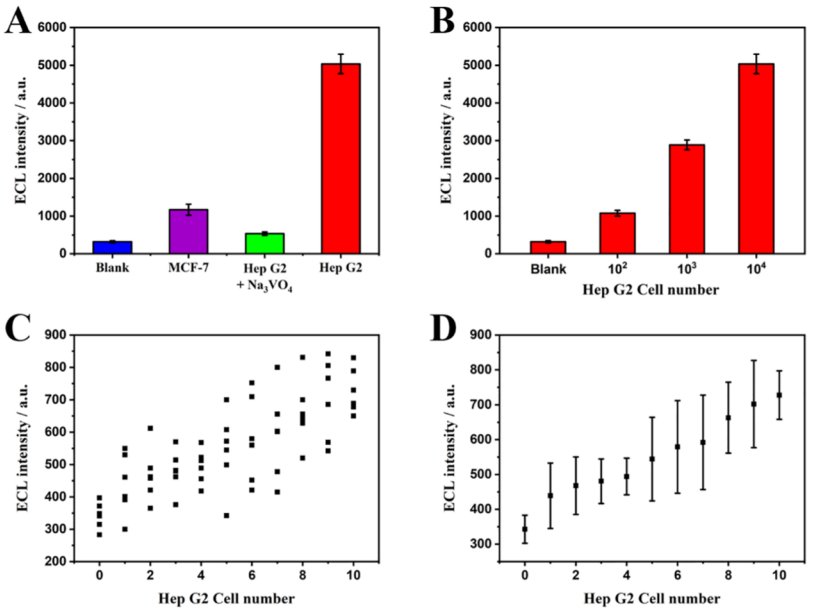

Figure 6. (A) ALP detection in different types of cells (10^4 MCF-7 cells, 10^4 Hep G2 cells + Na_3VO_4, 10^4 Hep G2 cells). (B) ALP detection in different quantities of Hep G2 cells. (C) Scatter plot of the ECL responses of 0−10 Hep G2 cells. (D) Relationship between the ECL intensities and the number of Hep G2 cells (the error bar is the standard deviation of six experimental samples).

CONCLUSIONS

In summary, we proposed an ultrasensitive electrochemiluminescence biosensor based on a closed bipolar electrode for the detection of ALP. Combined with the signal amplification strategy of ALP enzyme catalysis, this biosensor showed high sensitivity and specificity for ALP detection. As low as 0.005 fM ALP could be detected with a good linear range from 0.005 to 0.5 fM in the biosensor, which had a low detection limit of 3.7 aM. Most importantly, this biosensor had also been applied to the detection of ALP in a single Hep G2 cell and showed potential for ALP detection in single cell electrochemical detection. The developed biosensor could be utilized to detect many other biological molecules and expected to be applied in single biomolecule detection or single cell analysis. Also, the constructed BPE−ECL system could realize anode oxidation and anode ECL signal output, which broadened the application range of the BPE−ECL system.

ASSOCIATED CONTENT

Supporting Information

The Supporting Information is available free of charge at https://pubs.acs.org/doi/10.1021/acs.analchem.0c04517.

Figure S1, optimization of the driving voltage; Figure S2, optimization of detection conditions; Figure S3, ALP detection by extending the experimental conditions; Figure S4, *p*-AP detection; Table S1, comparison of this method and some other reported methods with ECL biosensor based on a closed bipolar electrode (PDF)

AUTHOR INFORMATION

Corresponding Author

Zhi-Ling Zhang − *College of Chemistry and Molecular Sciences, Wuhan University, Wuhan 430072, P. R. China;* orcid.org/0000-0001-7807-2264; Phone: 0086-27-68756759; Email: zlzhang@whu.edu.cn; Fax: 0086-27-68754067

Authors

Xiao-Yan Yang − *College of Chemistry and Molecular Sciences, Wuhan University, Wuhan 430072, P. R. China*

Yi-Yan Bai − *College of Chemistry and Molecular Sciences, Wuhan University, Wuhan 430072, P. R. China*

Yue-Yue Huangfu − *College of Chemistry and Molecular Sciences, Wuhan University, Wuhan 430072, P. R. China*

Wen-Jing Guo − *College of Chemistry and Molecular Sciences, Wuhan University, Wuhan 430072, P. R. China*

Yan-Ju Yang − *College of Chemistry and Molecular Sciences, Wuhan University, Wuhan 430072, P. R. China*

Dai-Wen Pang − *College of Chemistry and Molecular Sciences, Wuhan University, Wuhan 430072, P. R. China;* orcid.org/0000-0002-7017-5725

Complete contact information is available at: https://pubs.acs.org/10.1021/acs.analchem.0c04517

Notes

The authors declare no competing financial interest.

ACKNOWLEDGMENTS

This work was supported by the National Natural Science Foundation of China (21775111, 21535005, and 22074107).

REFERENCES

(1) Mavré, F.; Anand, R. K.; Laws, D. R.; Chow, K. F.; Chang, B. Y.; Crooks, J. A.; Crooks, R. M. *Anal. Chem.* **2010**, *82*, 8766−8774.

(2) Zhang, X.; Chen, C.; Li, J.; Zhang, L.; Wang, E. *Anal. Chem.* **2013**, *85*, 5335−5339.

(3) Baek, S.; Kwon, S. R.; Yeon, S. Y.; Yoon, S. H.; Kang, C. M.; Han, S. H.; Lee, D.; Chung, T. D. *Anal. Chem.* **2018**, *90*, 4749−4755.

(4) Zhang, H. R.; Wang, Y. Z.; Zhao, W.; Xu, J. J.; Chen, H. Y. *Anal. Chem.* **2016**, *88*, 2884−2890.

(5) Qin, X.; Yu, J.; Jiao, M.; Shan, X.; Xian, X.; Wang, D.; Tao, N. *Anal. Chem.* **2020**, *92*, 799−805.

(6) Zhang, X.; Zhai, Q.; Xing, H.; Li, J.; Wang, E. *ACS Sens.* **2017**, *2*, 320−326.

(7) Lin, Y.; Huang, X.; Zhang, Y.; Chen, D.; Wang, J.; Luo, F.; Guo, L.; Qiu, B.; Lin, Z. *ChemElectroChem* **2019**, *6*, 827−833.
(8) Khoshfetrat, S. M.; Khoshsafar, H.; Afkhami, A.; Mehrgardi, M. A.; Bagheri, H. *Anal. Chem.* **2019**, *91*, 6383−6390.
(9) Han, Z.; Shu, J.; Liang, X.; Cui, H. *Anal. Chem.* **2019**, *91*, 12260−12267.
(10) Li, L.; Chen, Y.; Zhu, J. J. *Anal. Chem.* **2017**, *89*, 358−371.
(11) Zhou, Y.; Yan, D.; Wei, M. *J. Mater. Chem. C* **2015**, *3*, 10099−10106.
(12) Wu, M. S.; Yuan, D. J.; Xu, J. J.; Chena, H. Y. *Chem. Sci.* **2013**, *4*, 1182−1188.
(13) Chow, K. F.; Mavré, F.; Crooks, R. M. *J. Am. Chem. Soc.* **2008**, *130*, 7544−7545.
(14) Wu, M. S.; Yuan, D. J.; Xu, J. J.; Chen, H. Y. *Anal. Chem.* **2013**, *85*, 11960−11965.
(15) Wang, Y. Z.; Xu, C. H.; Zhao, W.; Guan, Q. Y.; Chen, H. Y.; Xu, J. J. *Anal. Chem.* **2017**, *89*, 8050−8056.
(16) Zhai, Q.; Zhang, X.; Han, Y.; Zhai, J.; Li, J.; Wang, E. *Anal. Chem.* **2016**, *88*, 945−951.
(17) Anderson, T. J.; Defnet, P. A.; Zhang, B. *Anal. Chem.* **2020**, *92*, 6748−6755.
(18) Chang, B. Y.; Chow, K. F.; Crooks, J. A.; Mavré, F.; Crooks, R. M. *Analyst* **2012**, *137*, 2827−2833.
(19) Shi, H. W.; Zhao, W.; Liu, Z.; Liu, X. C.; Xu, J. J.; Chen, H. Y. *Anal. Chem.* **2016**, *88*, 8795−8801.
(20) Arora, A.; Eijkel, J. C. T.; Morf, W. E.; Manz, A. *Anal. Chem.* **2001**, *73*, 3282−3288.
(21) Zhan, W.; Alvarez, J.; Crooks, R. M. *J. Am. Chem. Soc.* **2002**, *124*, 13265−13270.
(22) Lu, S. M.; Peng, Y. Y.; Ying, Y. L.; Long, Y. T. *Anal. Chem.* **2020**, *92*, 5621−5644.
(23) Lu, H. J.; Zhao, W.; Xu, J. J.; Chen, H. Y. *Biosens. Bioelectron.* **2018**, *102*, 624−630.
(24) Wu, M. S.; Xu, B. Y.; Shi, H. W.; Xu, J. J.; Chen, H. Y. *Lab Chip* **2011**, *11*, 2720−2724.
(25) Zhang, X.; Li, J.; Jia, X.; Li, D.; Wang, E. *Anal. Chem.* **2014**, *86*, 5595−5599.
(26) Shi, H. W.; Zhao, W.; Liu, Z.; Liu, X. C.; Wu, M. S.; Xu, J. J.; Chen, H. Y. *Talanta* **2016**, *154*, 169−174.
(27) Li, X.; Du, Y.; Wang, H.; Ma, H.; Wu, D.; Ren, X.; Wei, Q.; Xu, J.-J. *Anal. Chem.* **2020**, *92*, 12693−12699.
(28) Zhang, N.; Gao, H.; Xu, C. H.; Cheng, Y.; Chen, H. Y.; Xu, J. J. *Anal. Chem.* **2019**, *91*, 12553−12559.
(29) Wu, J.; Chumbimuni-Torres, K. Y.; Galik, M.; Thammakhet, C.; Haake, D. A.; Wang, J. *Anal. Chem.* **2009**, *81*, 10007−10012.
(30) Möller, R.; Powell, R. D.; Hainfeld, J. F.; Fritzsche, W. *Nano Lett.* **2005**, *5*, 1475−1482.
(31) Lin, T.; Wu, Y.; Li, Z.; Song, Z.; Guo, L.; Fu, F. *Anal. Chem.* **2016**, *88*, 11022−11027.
(32) Zhou, C. H.; Zhao, J. Y.; Pang, D. W.; Zhang, Z. L. *Anal. Chem.* **2014**, *86*, 2752−2759.
(33) Wu, Z.; Zhou, C. H.; Pan, L. J.; Zeng, T.; Zhu, L.; Pang, D. W.; Zhang, Z. L. *Anal. Chem.* **2016**, *88*, 9166−9172.
(34) Wu, Z.; Guo, W. J.; Bai, Y. Y.; Zhang, L.; Hu, J.; Pang, D. W.; Zhang, Z. L. *Anal. Chem.* **2018**, *90*, 1683−1690.
(35) Wu, M. S.; Liu, Z.; Shi, H. W.; Chen, H. Y.; Xu, J. J. *Anal. Chem.* **2015**, *87*, 530−537.
(36) Zhang, J. D.; Lu, L.; Zhu, X. F.; Zhang, L. J.; Yun, S.; Duanmu, C. S.; He, L. *ACS Sens.* **2018**, *3*, 2351−2358.

https://dx.doi.org/10.1021/acs.analchem.0c04517
Anal. Chem. 2021, 93, 1757−1763